

# Synthesis of Ni-Fe-Al Heusler alloys and study of their microstructure and FSMA nature

Kuldeep Kargeti<sup>1\*</sup>, Ankit Kargeti<sup>2</sup> and PK Mukhopadhyay<sup>3</sup>

<sup>1</sup>M.Sc. II Sem. (Physics), School of Physical Sciences, Doon University, Dehradun

<sup>2</sup>M.Sc. IV Sem. (Physics), Invertis Institute of Applied Science and Humanities, Invertis University, Bareilly

<sup>3</sup>Laboratory of Condensed Matter Physics, SN Bose National Centre for Basic Science, Kolkata

**Abstract:** Ferromagnetic shape memory alloys (FSMA) exhibit Austenite – Martensite phase transformation which is a diffusionless structural transformation from a high temperature cubic phase to a lower temperature lower symmetry phase, like orthorhombic, monoclinic etc. These structural transformations are generally studied through resistivity, magnetization etc measurements. In this paper we discuss the results of our work on a Ni based FSMA alloy having composition  $\text{Ni}_{60}\text{Fe}_{19}\text{Al}_{21}$  in order to find the shape memory effect closer to the room temperature. This compound can be a very useful substitute for other present systems in the category of smart materials. In addition to the conventional methods, we have also investigated the microstructure, AC resistivity as well as magnetic properties of this compound.

**Keywords:** Shape memory alloy, Smart materials, Microstructure, Heusler alloys.

## 1. INTRODUCTION

### 1.1 Heusler Alloys

Heusler alloys are inter-metallic compounds with fcc structure characterized by the chemical formula  $\text{X}_2\text{YZ}$  (Full Heusler alloy) and  $\text{XYZ}$  (half Heusler alloy), where X and Y are transition metal atoms and Z lies in the p-block of the periodic table. These alloys exhibit ferromagnetism, anti-ferromagnetism, superconductivity, thermoelectricity and magneto resistance. The first Heusler compound was discovered by the German scientist Heusler in 1930, who showed that in these compounds or alloys, magnetism varies with heat treatment. Some of the Heusler alloys show the properties of Ferromagnetic Shape Memory Alloys (FSMA). These are composed of Ni, Mn, Ga, Al, Fe, Co, Ge, Pd (like  $\text{Ni}_2\text{MnAl}$ ,  $\text{Ni}_2\text{MnGa}$ ,  $\text{Ni}_2\text{MnIn}$ ,  $\text{Ni}_2\text{MnSn}$ ,  $\text{Ni}_2\text{MnSb}$ , where Ni is X, Mn is Y, and Al, Ga, In, Sn, Sb are Z). The size and shape of FSMA can be altered by an external magnetic field. (see reference [1-16])

### 1.2 Ferromagnetic Shape Memory Alloys

When the temperature of the martensitic phase is increased, it converts into the Austenite Phase; this transformation involves a transition from the tetragonal structure of the martensitic to the cubic structure of the austenite (See Figure 1). Ferromagnetic Shape Memory (FSM) effect usually occurs in the low temperature Martensitic phase of the alloy. FSMA's undergo changes in their original structure when placed in an external magnetic field or alternatively by the effect of heat. For example, the shape of a FSMA changes in the presence of an external magnetic field and the original shape is recovered when the field is removed. A similar effect also occurs under heat treatment. The recovery

---

\*kuldeepkargeti@gmail.com

of the original shape by cooling or removal of the magnetic field occurs because the low temperature structure of FSMA has twin variants. During the application of magnetic field, as is common in several magneto elastic smart materials, there occurs simultaneous rotation of magnetic moments and reorientation of twin variants, (refer to the Figure 1). In the presence of external magnetic field, the boundaries between the variants are shifted and the domains align along one direction. When the magnetic field is removed the original domain structure reappears.

Magnetic anisotropy (MI) plays a crucial role in determining the energy required to change the magnetic structure in FSMA. The strength of MI determines the maximum strain associated with the FSMA property and which can be used for applications like actuators, sensors, memory devices, magnetic cooling systems and next generation material for aerodynamics.

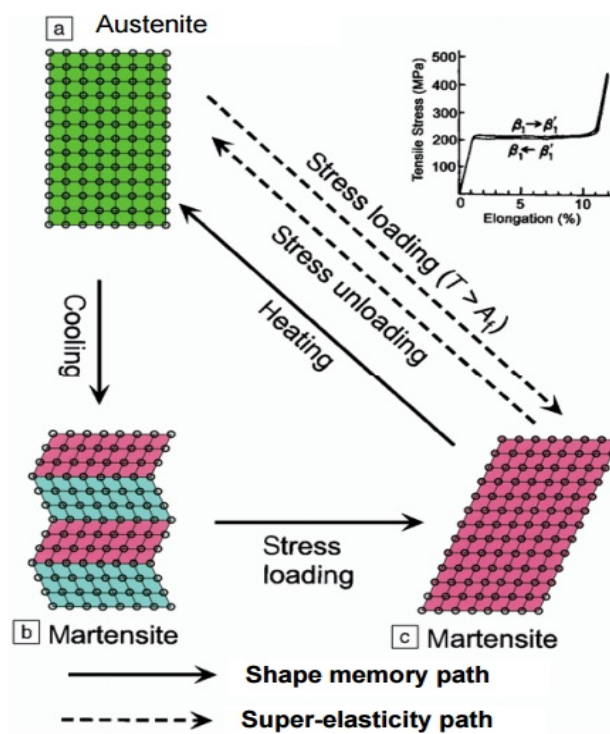


Figure 1–Schematic diagram showing the phase transformation of FSMA

## 2. SAMPLE PREPARATION

### 2.1 Weighing And Cutting

Approximately 2 grams of polycrystalline  $\text{Ni}_{60}\text{Fe}_{19}\text{Al}_{21}$  alloy was prepared using an Arc melting furnace. High purity of raw elements Nickel (99.99%), Fe (99.99%) and Al (99.99%) were used. For this sample, Ni is around 1.3684 gm, Fe is around 0.4163 gm and Al is around 0.2217 gm. The sample is cut by Stanley Bolt cutter.

## 2.2 Melting

The alloy is melted in a Vacuum Arc Melting Furnace (See Figure 2). First we cleaned the glass chamber by acetone and then we made vacuum inside chamber (glass) around  $10^{-3}$  pa. Then the weighed sample was kept on a copper crucible and was melted in an arc furnace three times under the flow of argon gas. The system was simultaneously cooled by the chilling water. The reason for melting three times is to improve the homogeneity of the alloy.

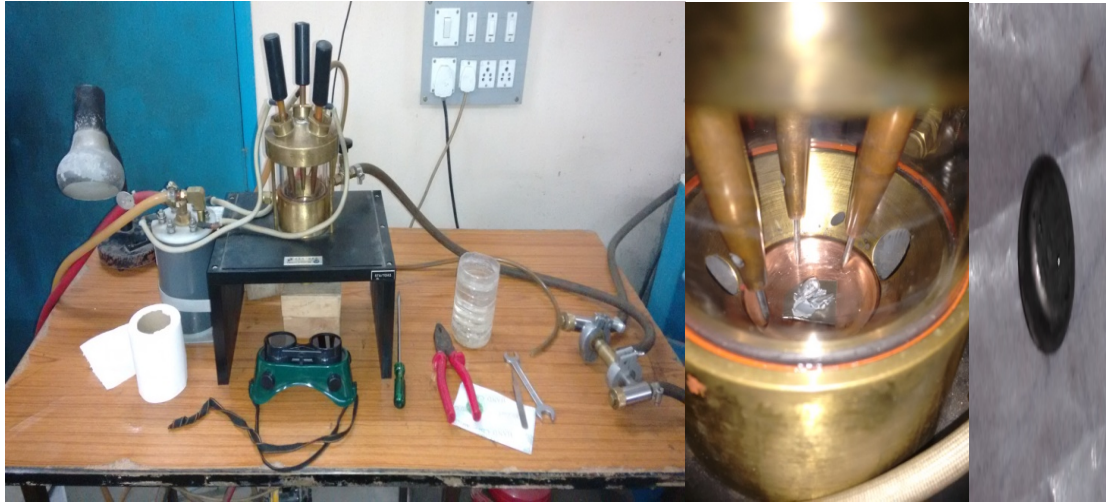


Figure 2-Vacuum Arc Melting Furnace set up and copper hearth

## 2.3 Cutting, Annealing, Polishing

Next step is to cut the arc melted sample into three parts using an anisomet diamond cutter, which took approximately 5 to 6 hours under a constant rpm (3rpm). The three parts were then polished with a polishing machine for nearly 2 hours for each part. Then two parts are put in a sealed Quartz ampule for heat treatment to increase the homogeneity of the sample further. The next step is to anneal the sample at  $1000^{\circ}\text{C}$  for 48 hours. This is done through a resistive furnace whose temperature is fixed at the desired value for a given prescribed time. This is followed by a rapid quenching in cooled water. This was necessary to decrease the amount of undesired gamma phase and to give better results in our experiments. The annealed sample is then polished with the help of a polishing machine for 1 hour approximately for both the parts. The sample is then placed over the polishing cloth which is rayon fine and 1 micron in grit size, and chromium oxide powder was used to remove the dust from the sample surface. This is needed to get a more shinier surface as well as to get sharp edges. Now the sample is ready for different characterization experiments.

## 3. SAMPLE ANALYSES:

### 3.1 Resistivity Measurement

Resistivity measurement is done through a custom designed four-probe setup starting from a low temperature of 100 K to a maximum temperature of 300 K. This experimental set up consists of the four probe arrangement, sample holder, constant current generator, power supply and digital screen for measuring voltage and current across the probes (See Figure 3).

Since the resistivity  $\rho$  is  $R \cdot A / L$ , we measured the length  $L$  of the sample as 2.5 mm, width of the sample as 0.8 mm (area  $A$  is  $2.00 \text{ mm}^2$ ). From the experiment we found the resistance  $R$  of the sample with current fixed at AC frequency of 111.11 Hz and Voltage around 5 Volts with the known standard resistance  $35.5 \Omega$ . The values of the  $\rho$  is obtained as a function of temperature ranging from 4K to 300K.



Figure 3. Indigenously designed set up to measure resistivity using ac four probe method

### **3.2 XRD Measurement**

One part of the sample is used for the XRD Measurement, carried out by Rigaku X-Ray Diffractometer at 2deg/min. The measurements were carried out from 10 to 90 degrees, which is based on Bragg's diffraction equation  $2d \sin\theta = n\lambda$ , where the angle  $\theta$  is the diffraction angle and  $\lambda$  is the wavelength of the x-ray beam and  $d$  is the spacing between the two atomic layers.

### **3.3 FESEM**

FESEM is Field Emission Scanning Electron Microscope, which is used to characterize the topological details of a fractured surface. It has a range of imaging from  $100 \mu\text{m}$  to  $5 \mu\text{m}$ , which is quite good for surface analyses.

## 4. RESULT

### 4.1 Data Analyses

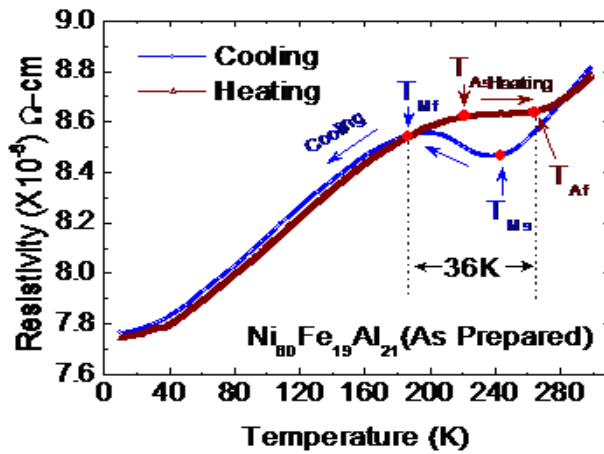


Figure 4 – Structural transformation under the temperature changes.

In Figure 4, we show the temperature dependence of resistivity in the range from 4K-300K. We find the austenitic to martensitic transition while heating and Martensitic transformation while cooling. The Martensitic transformation process starts below the room temperature at  $M_s$  (242 K) and finish at  $M_f$  (188 K). When we heat the sample upto the room temperature we found the Austenitic transformation starts at  $A_s$  (221 K) and finish at temperature  $A_f$  (264 K). To confirm that there is Austenitic to Martensitic transformation, we measured the magnetization of the sample in a constant field of 150 Oe in the temperature range 80 K to 400 K.

Through the XRD measurements we were able to characterize the structure of the alloy (See Figure 5). The XRD peaks were matched with the Full Prof Software and also with JCPD data base system. It has fcc austenite structure with the peaks at (110) and (211), at different positions and body centered cubic structure with peaks at different positions (111), (222) (see below). In addition there are some other peaks associated with gamma rich phases. These observations confirm the presence of austenitic phase and martensitic phase.

These observed XRD peaks clearly indicate that the as prepared alloy possess two phases beta ( $\beta$ ) and gamma ( $\gamma$ ) at room temperature. The Single phase ( $\beta$ ) Ni-Fe-Al alloy shows very sharp martensitic transition, but has extremely low ductility at room temperature. The presence of the second phase ( $\gamma$ ) with disordered fcc structure as a solid solution in NiFeAl system renders the  $\beta$ -phase ductile at room temperature and makes it useful for practical applications. ( see [14])

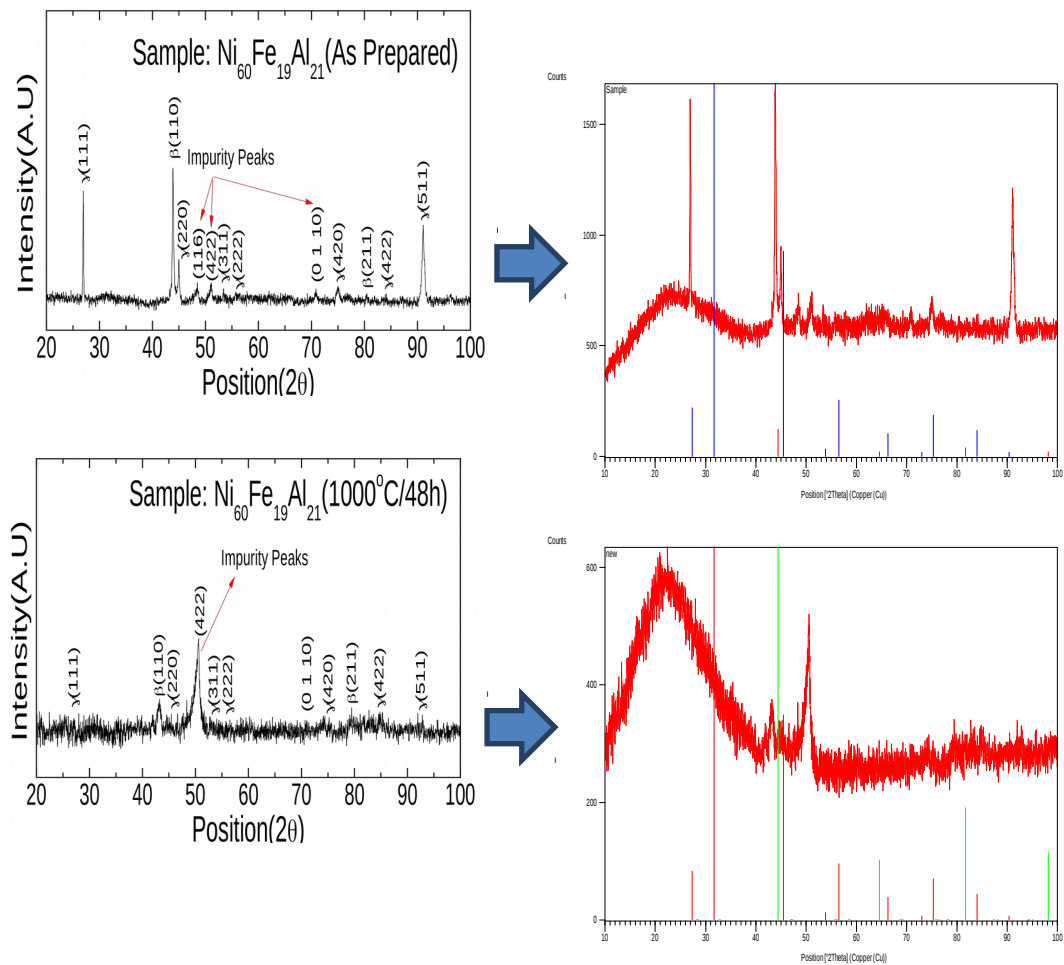


Figure 5- XRD observation for as prepared and annealed sample

#### 4.2 FESEM Analysis

With the FESEM we are able to find the two phases in the NiFeAl alloy and this has been matched with the work done on FSMA NiFeAl alloy before. (see [15]) We have also confirmed this from our XRD analyses. In Figure 6a and 6b we show the FESEM images for as prepared sample and for the sample annealed at 1000° C. The Curie temperature of the unannealed sample is low, around 123K. Annealing the sample removes defects and is expected to bring the transition temperature range closer to the room temperature. As we anneal the sample at 1000 degree Celsius we expect the Curie temperature for the system to increase and come closer to the room temperature. (see reference [16]) We have also seen that annealing makes the structural transition from austenitic phase to martensitic phase closer to the range of room temperature around 300K. Therefore it is clear that annealing the sample is very important.



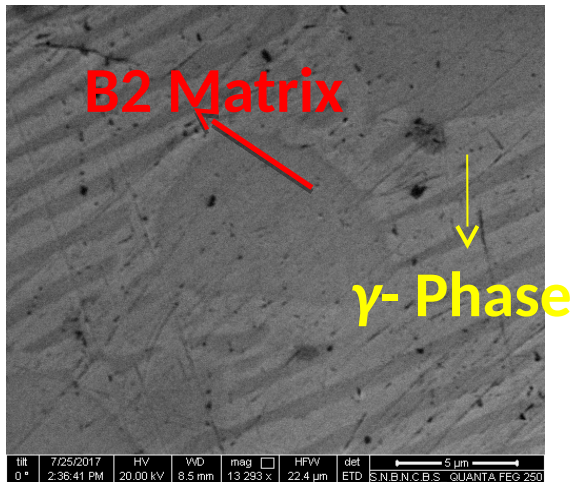


Fig 6a SEM of samples of as prepared

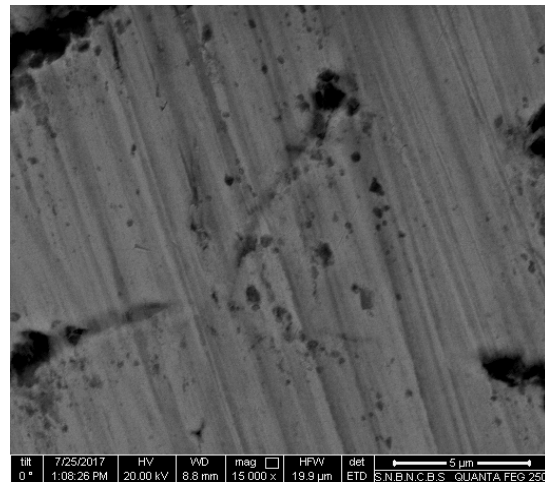


Fig 6b SEM of samples annealed at 1000°C/48h

## 5. CONCLUSION

In this paper we have focused on the synthesis and characterization study of the FSMA  $\text{Ni}_{60}\text{Fe}_{19}\text{Al}_{21}$  alloy, which is an excellent alternate system for the commonly used FSMA, NiMnGa. In contrast to the low ductility of the Ga system, the Fe alloy has high ductility and it is not brittle. This makes the  $\text{Ni}_{60}\text{Fe}_{19}\text{Al}_{21}$  alloy suitable as ferromagnetic shape memory alloy for application as actuators and sensors. In order to understand the full range of its properties one has to perform other measurements such as Differential Scanning Calorimetry and low temperature XRD. Further study will involve annealing the system at different temperatures and study how the FSM properties change with this in order to optimize the system for application.

## 6. REFERENCES

- [1] P. K. Mukhopadhyay and S. N. Kaul: Appl. Phys. Lett. **92**, pp 101924 (2008).
- [2] B. Rajini Kanth, P.K. Mukhopadhyay and S. N. Kaul: Adv. Materials Research **52** pp 129-133 (2008).
- [3] R. K. Singh and R. Gopalan: Adv. Materials Research Vol. **52** pp 57-62 (2008).
- [4] B. Rajini Kanth, N.V. Ramarao, A. K. Panda, R. Gopalan, A. Mitra, P. K. Mukhopadhyay: Jour. of Alloys and Compounds **491** 22 (2010).
- [5] Madhusmita Baral and Aparna Chakrabarti: arXiv:1701.08282v2 (cond-mat. matl-sci) 15/06/2017.
- [6] V. A. Cherenko, E. Cesari, J. Pons, C. Segui, Jour. of Materials Res. **15** (2000) 1496.
- [7] R. Kainuma, M. Ise, C-C. Jia, H. Ohtani and K. Ishida, Intermetallics **4** (1996) S151.
- [8] K. Oikawa, T. Ota, F. Gejima, T. Ohmor, R. Kainuma, K. Ishida, Materials. Trans **42** (2001) 2472.
- [9] K. Pushpanathan, R. Senthur Pandi, R. Chokkalingam, M. Mahendran, Advanced Material Research **52** pp 121-128 (2008).
- [10] S. N. Kaul, B. Annie D'Santhosini, A. C. Abhayankar, Applied Phys. Letter. **89** (2006), 093119.
- [11] Sarowar Hussain, P. K. Mukhopadhyay, B. Rajini Kanth, Springer 21/07/2017.
- [12] Chengbao Jiang, <https://www.researchgate.net/publication/223333223>.
- [13] F. X. hu, J. Shen, J. Wang, J. R. sun, B. G. Shen: <https://doi.org/10.1016/j.jmmm.2009.03.047>
- [14] B. Rajini Kanth, P.K. Mukhopadhyay, <https://doi.org/10.1016/j.matpr.2016.11.056>.
- [15] H. Okumura, K. Uemura, <https://doi.org/10.1016/j.intermet.2011.06.015>.
- [16] K. Oikawa, T. Omori, R. Kainuma, J. Magn. Magn. Mater, **272** p. 2043-2044 (2004).